ChemComm

Accepted Manuscript

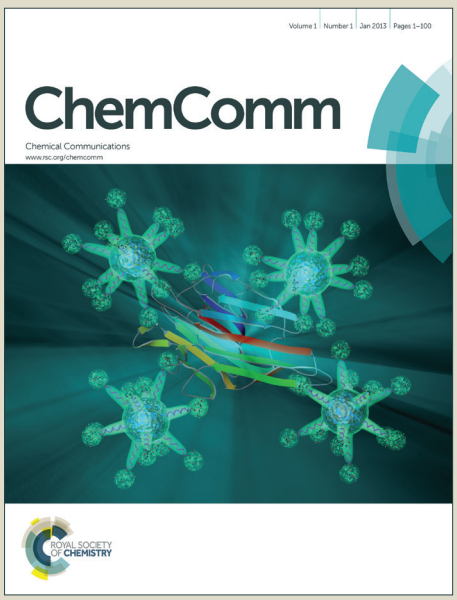

ROYAL SOCIETY OF CHEMISTRY

www.rsc.org/chemcomm

ChemComm

RSCPublishing

COMMUNICATION

Single-Base Mismatch Discrimination by T7 Exonuclease with Target Cyclic Amplification Detection

Cite this: DOI: 10.1039/xoxxoooooox

Received ooth January 2012,
Accepted ooth January 2012

DOI: 10.1039/xoxxoooooox

www.rsc.org/

Zhen-Kun Wu, Dian-Ming Zhou, Zhan Wu*, Xia Chu, Ru-Qin Yu and Jian-Hui Jiang*

T7 exonuclease is reported for the first time to have high specificity in discriminating single-base mismatch and utilized for developing a target cyclic amplification biosensor strategy for sensitive SNP detection based on graphene oxide quenching of uncleaved probes.

Single-nucleotide polymorphism (SNP) detection is of great importance for clinical diagnostics because of its close association with many diseases such as tumours and genetic disorders.[1] SNP detection typically relies on a mechanism for allele discrimination. While allele-specific hybridization works for SNP detection, complicated optimization and stringent control of the assays are required.[2] Hence, enzymatic discrimination of single-base mismatch becomes a prevailed option for SNP detection due to its robustness and specificity. Existing mechanisms for allele discrimination include ligase based ligation,[3] polymerase based nucleotide incorporation,[4] primer extension,[5] proof-reading[6] and endonuclease based cleavage.[7] Our group[8] and others[9] have adapted these mechanisms to design a variety of biosensor strategies for SNP genotyping. However, a low-cost, robust and selective strategy for SNP detection still remains an unmet challenge.

T7 exonuclease hydrolyzes duplex DNA in the direction of 5' to 3' from 5' phosphoryl or 5' hydroxyl nucleotides. It shears from the 5' termini or at gaps and nicks of double-strand DNA. It also has been reported to degrade DNA and RNA from DNA/RNA hybrids in the 5' to 3' direction.[10] Herein we report for the first time that T7 exonuclease has very high specificity in discriminating single-base mismatch with a reaction rate ratio of ~26 for perfect match over single-base mismatch. This new allele discrimination mechanism is exploited for developing a target cyclic amplification biosensor strategy for sensitive SNP detection. By using graphene oxide (GO) based selective quenching of uncleaved probes, the biosensor strategy provides a low-cost platform for sensitive, selective SNP detection.

The allele-specific discrimination mediated by T7 exonuclease was firstly investigated (Fig. S1, ESI†). Probe 1 (Table S1, ESI†) with a 5-carboxy fluorescein (FAM) fluorophore at 5' terminal and a dabcyl quencher in adjacent nucleotides was designed and was perfect match to the mutant-type target while formed single-base mismatch to the wild-type target at 5' terminal. For the perfect match system, probe 1 will be hydrolysed successively into mononucleotides from 5' terminal by T7 exonuclease and the fluorescence of FAM will be recovered. For the single-base mismatch system, the mismatched base will prevent T7 exonuclease from degrading probe 1 and the fluorescence will remain be quenched by dabcyl. Because cyclical degradation of the input probe

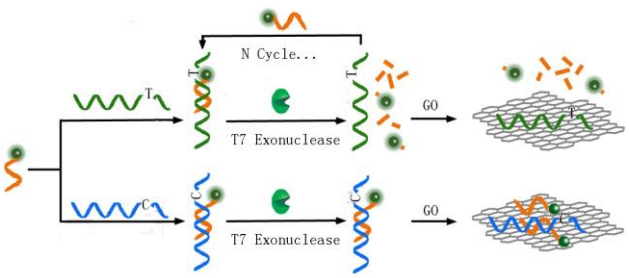

Scheme 1. Scheme for SNP detection based on T7 exonuclease with target cyclic amplification.

1 affords efficient amplification of the fluorescence signal, we are able to achieve high sensitivity in detecting the target DNA. Based on the above mechanism, a novel fluorescence SNP detection strategy was proposed by using GO as a "nanoquencher". It was reported that GO bound and quenched fluorophore-labeled single-stranded DNA but had less affinity to double-stranded DNA.[11] As illustrated in Scheme 1, probe 2 with FAM tag at 5' end is designed to perfectly complement the mutant-type target while form single-base mismatch to the wild-type target at 5' terminal. For the mutant-type target, T7 exonuclease facilitates a process of target recycling that rapidly shears probe 2, and produces numerous mononucleotides and short oligonucleotide fragments, after adding the GO, the production of digestion will not be adsorbed by GO, leading fluorescence to be reserved; while for the wild-type target, probe 2 will not be digested by T7 exonuclease, resulting fluorescence quenched after adding the GO.

To assess the ability of allele-specific discrimination by T7 exonuclease, we synthetized two model DNA sequences of human β-Thalassemia gene around IVSⅡ-654 mutation site (mutant-type target and wild-type target), a known C >T mutation highly

associated with β-Thalassemia.[12] Probe 1 is separately annealed with the mutant-type target and the wild-type target followed by adding T7 exonuclease, and the degradation reactions of probe 1 was studied via real-time fluorescence analysis. As shown in Figure 1A, for the wild-type target, a very weak fluorescence signal was observed after incubated for 3 hours, and it did not show appreciable time-dependent fluorescence intensity changes. In contrast, for the mutant-type target, the fluorescence signal increased rapidly, suggesting that probe 1 was effectively degraded by T7 exonuclease. The maximum cleavage velocity (ν_{max}) was calculated by the standard Michaelis-Menten equation and shown in Figure 1B. The ν_{max} of the perfect match system is about 26 times faster than that of the single-base mismatch system, indicating that T7 exonuclease has very high specificity in discriminating single-base matches. This single-base mismatch discrimination efficiency was comparable against those using high-specific ligases.[13]

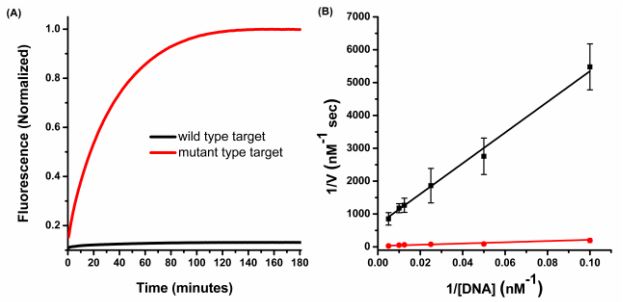

Figure 1. Comparison of the digestion rates of the mutant-type target and the wild-type target. (A) Fluorescence-based progress curves of the T7 exonuclease digestion reaction as a function of time. (B) Double reciprocal plot of the initial reaction velocity as a function of DNA concentration.

Feasibility of the developed strategy for single-base mismatch discrimination was investigated. GO nanosheets used in this experiment were characterized by atomic force microscopy (AFM). GO nanosheets showed a topological height of ~1.1 nm (Fig. S2, ESI†), a typical thickness for single-layered GO nanosheets.[14] As shown in Figure 2A, when incubating the probe 2 with wild-type target and mutant-type target separately, subsequently followed by addition of GO nanosheets, only weak fluorescence was observed, suggesting the fluorescence of FAM labelled to probe 2 was efficiently quenched by the GO nanosheets. When adding T7 exonuclease into the systems above, the fluorescence was remarkably enhanced for the perfect match system of probe 2 and mutant-type target, evidencing that the FAM fluorophore were not adsorbed on the surface of GO nanosheets, and confirming that probe 2 was digested by T7 exonuclease. However, no substantial fluorescence increase was achieved for the single-base mismatch system of probe 2 and wild-type target, implying the FAM fluorophore were adsorbed on the GO surface. Thus, the assumption that single-base mismatch at the 5' terminus can efficiently prevent the T7 exonuclease degrading the probe 2 is proved and confirmed.

Further verification regarding the single-base mismatch discrimination mechanism was conducted by Agarose gel electrophoresis. As shown in Figure 2B, double-stranded DNAs generated by the hybridization of probe 2 with wild-type target and mutant-type target respectively made two bright bands with the same mobility (lane 1 and 2). Adding T7 exonuclease into systems above, almost no change occurred to the bright band (lane 3) compared with that in lane 1, repeatedly implying that probe 2 was not digested by T7 exonuclease due to the single-base mismatch with the wild-type target at 5'end. In contrast, bright band with obvious migration shifts (lane 4) was observed, suggesting the probe 2 was degraded by T7 exonuclease and this bright band is only from the mutant-type target.

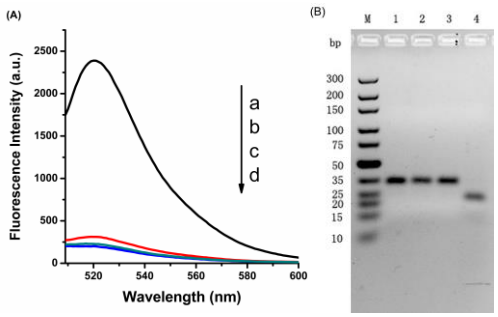

Figure 2. (A) Fluorescence Spectrum of SNP analysis. Line a, 20 nM mutant-type target and 80 nM probe 2 plus 0.26 U/μL T7 exonuclease and 5 ng/μL GO nanosheets, line b, 20 nM wild-type target and 80 nM probe 2 plus 0.26 U/μL T7 exonuclease and 5 ng/μL GO nanosheets, line c, 20 nM mutant-type target and 80 nM probe 2 plus 5 ng/μL GO nanosheets, line d, 20 nM wild-type target and 80 nM probe 2 plus 5 ng/μL GO nanosheets. (B) Agarose gel electrophoresis images for hybridization of DNA probe 2 and target DNA. Lane M, DNA marker; lane 1, 1 μM probe 2 and 1μM wild-type target; lane 2, 1 μM probe 2 and 1 μM mutant-type target; lane 3, 1 μM probe 2 and 1 μM wild-type target with 1 U/μL T7 exonuclease; lane 4, 1 μM probe 2 and 1 μM mutant-type target with 1 U/μL T7 exonuclease.

In order to optimize the concentration of T7 exonuclease, we adopted fluorescence signal ratio (F/F_0, signal from the mutant target divided by that from the wild type) as the measure (Fig. S3, ESI†). It was observed that the fluorescence signal ratio displayed a peak-shape dependency on the concentration of T7 exonuclease with a maximum achieved using 0.26 U/μL T7 exonuclease. Thus, this concentration of T7 exonuclease was used throughout the subsequent experiments.

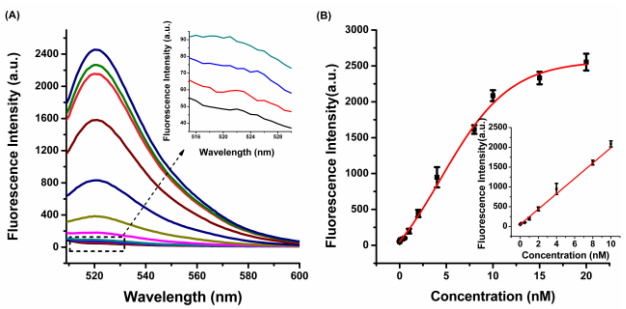

Figure 3. (A) Fluorescence spectrum of the probe 2 (80 nM) with different concentration of the mutant-type target (0, 0.01, 0.05, 0.1, 0.5, 1, 2, 4, 8, 10, 15, 20 nM, from bottom to top) was measured with 494 nm excitation wavelength. (B) Fluorescence intensity at 520 nm versus the concentration of the mutant-type target of this SNPs assay. Inset: linear relationship between fluorescence intensity and mutant-type target concentration. Error bars are standard deviation of three repetitive experiments.

In order to investigate the quantitative nature of the single-base discrimination technique, the mutant-type target of varying concentrations were measured using fluorescence spectra. As shown in Figure 3A, the fluorescence peaks dynamically increased with increasing concentration of the mutant-type target within the range from 0 to 20 nM. The fluorescence intensity versus mutant-type targets concentration showed a linear correlation with mutant-target concentration range from 10 pM to 10 nM, as shown in Figure 3B. The detection limit

was estimated to be 4 pM according to the 3σ rule. The performance of the proposed method was compared with other reported methods (Table S2, ESI†), demonstrating that this biosensor exhibited low detection limit and achieved high sensitivity. The relative standard deviations (RSDs) of fluorescence intensity were 3.6%, 2.8%, 5.3% and 3.7%, in four repetitive assays of 10 pM, 100 pM, 500 pM and 10 nM mutant-type target, exhibiting excellent reproducibility due to simple operations. The developed strategy offered advantages in high signal-to-background ratio and wide dynamic response range and it could be more robust, cost-efficient, readily automated, because of its homogeneous and fluorescence-based detection format.

Further results from detecting mixtures of mutant-type targets and wild-type targets were investigated (Fig. S4, ESI†). The mixed DNA samples were prepared by mixing mutant-type target and wild-type target of different ratios from 0% to 100%, and total concentration of wild-type and mutant-type analytes is 20 nM. One can observed that the fluorescence signals were dynamically enhanced with the increasing of the mutant-target from 0 % to 100% in mixed DNA samples. This experiment results demonstrated that the technique afforded extremely high specificity, which might be a potential alternative as an effective mutation detection technology for solid tumor-based cancer research.

The single-base mismatch discrimination technique was further validated using human genomic DNA sample with point mutant (C > T) at IVS Ⅱ-654 site in the beta-thalassemia gene. Six genomic samples were collected. Polymerase chain reaction (PCR) was performed on these samples to obtain 373-base-pair amplicons. The PCR amplicons were confirmed by agarose gel assay (Fig. S5, ESI†) and subsequently utilized for mutation detection by using the developed technique (Fig. S6, ESI†). It was observed that, for samples 3, 4, 5 and 6, fluorescence signals were significantly greater than the background response, implying that those four samples are of mutant-type. While sample 1 and 2 gave fluorescence signals comparable to the background response, suggesting that those two sample are of wild-type. The identified gene types were consistent with the sequence data, demonstrating that the developed method holds the potential for SNP detection of genomic DNA samples.

In conclusion, we reported for the first time that T7 exonuclease can efficiently discriminate the perfectly matched base pairs from the single-base mismatched pairs with a discrimination ratio of ~26. On the basis of this new allele discrimination mechanism, a target cyclic amplification biosensor strategy was developed for SNP detection. This strategy is validated to exhibit superb robustness, high signal-to-background ratio, desirable sensitivity and selectivity, low cost, and simple. Furthermore, different sequence DNA probes with distinct fluorescence tags can be designed, which should allow the strategy to be useful for multiplex assays. In light of these advantages, this new allele discrimination mechanism can be expected to hold considerable potential for genomic research.

This work was supported by NSFC (21025521, 21405040, 21190041, 91317312, 21205034, 21307029, 21221003), National Key Basic Research Program (2011CB911000) and Fundamental Research Funds for Central University (531107040687).

Notes and references

State Key Laboratory of Chemo/Bio-Sensing and Chemometrics, College of Chemistry and Chemical Engineering, Hunan University, Changsha, 410082, P. R. China, Tel: 86-731-88664085; Fax :86-731-88821848; E-mail: wuzhan1002@gmail.com; jianhuijiang@hnu.edu.cn

† Electronic Supplementary Information (ESI) available: Experimental details and additional Figures. See DOI: 10.1039/b000000x/

1 (a) E. N. Imyanitov, *Hum. Genet.*, 2009, **125**, 239-246; (b) M. D. Gobbi, V. Viprakasit, J. R. Hughes, C. Fisher, V. J. Buckle, H. Ayyub, R. J. Gibbons, D. Vernimmen, Y. Yoshinaga, P. D. Jong, J. F. Cheng, E. M. Rubin, W. G. Wood, D. Bowden and D. R. Higgs, *Science*, 2006, **312**, 1215-1217.

2 (a) A. C. Syvanen, *Nat. Rev. Genet*., 2001, **12**, 930-942; (b) B. W. Kirk, M. Feinsod, R. Favis, R. M. Kliman and F. Barany, *Nucleic. Acids. Res*., 2002, **15**, 3295-3311.

3 (a) Z. Xiao, P. C. Lie, Z. Y. Fang, L. X. Yu, J. H. Chen, J. Liu, C. C. Ge, X. M. Zhou and L. W. Zeng, *Chem. Commun*., 2012, **48**, 8547-8549; (b) J. S. Li, S. Schachermeyer, Y. Wang, Y. D. Yin and W. W. Zhong, *Anal. Chem*., 2009, **81**, 9723-9729; (c) Y. Q. Cheng, Q. Du, L. Y. Wang, H. L. Jia and Z. P. Li, *Anal. Chem*., 2012, **84**, 3739-3744.

4 F. Chen, E. A. Gaucher, N. A. Leal, D. Hutter, S. A. Havemann, S. Govindarajan, E. A. Ortlund and S. A. Benner, *Proc. Natl. Acad. Sci.*, 2010, **107**, 1948-1953.

5 (a) H. Zhou, S. J. Xie, S. B. Zhang, G. L. Shen, R. Q. Yu and Z. S. Wu, *Chem. Commun*., 2013, **49**, 2448-2450; (b) X. R. Duan, S. Wang and Z. P. Li, *Chem. Commun*., 2008, 1302-1304; (c) J. Gaster, G. Ranqam and A. Marx, *Chem. Commun*., 2007, 1692-1694.

6 (a) P. Cahill, M. Bakis and J. Hurley, et al, *Genome Res*., 2003, **13**, 925-931; (b) C. L. Ling, J. Zhang, S. S. Sommer and K. Li, *J. Biochem. Mol. Biol*., 2005, **38**, 24-27.

7 S. Shin, B. Y. Won, C. Jung, S. C. Shin, D. Y. Cho, S. S. Lee and H. G. Park, *Chem. Commun*., 2011, **47**, 6611-6613.

8 (a) Y. Huang, Y. L. Zhang, X. M. Xu, J. H. Jiang, G. L. Shen and R. Q. Yu, *J. Am. Chem. Soc*., 2009, **131**, 2478-2480; (b) H. Q. Wang, W. Y. Liu, Z. Wu, L. J. Tang, X. M. Xu, R. Q. Yu and J. H. Jiang, *Anal. Chem*., 2011, **86**, 1883-1889.

9 J. H. Chen, J. Zhang, J. Li, F. F. Fu, H. H. Yang and G. N. Chen, *Chem. Commun*., 2010, **46**, 5939-5941.

10 (a) C. Kerr and P. D. Sadowski, *J. Biol. Chem*., 1972, **247**, 305-318; (b) K. Shinozaki and T. Okazaki, *Nucl. Acids. Res*., 1978, **5**, 4245-4261.

11 (a) L. Lin, Y. Liu, X. Zhao and J. H. Li, *Anal. Chem*., 2011, **83**, 8396-8402; (b) B. W. Liu, Z. Y. Sun, X. Zhang and J. W. Liu, *Anal. Chem*., 2013, **85**, 7987-7993.

12 K. M. Chan, M. S. Wong, T. K. Chan and V. Chan, *Br. J. Haematol.*, 2004, **124**, 232-239.

13 U. Landegren, R. Kaiser, J. Sanders and L. Hood, *Science*, 1988, **241**, 1077-1080.

14 H. Pei, J. Li, M. Lv, J. Y. Wang, J. M. Gao, J. X. Lu, Y. P. Li, Q. Huang, J. Hu and C. H. Fan, *J. Am. Chem. Soc*., 2012, **134**, 13843-13849.